BMC Pregnancy and Childbirth

RESEARCH

Open Access

Correlation between fetal-placental doppler indices and maternal cardiac function in pregnant women with late-Onset preeclampsia or fetal growth restriction

Yiling Chen[1], Meihong Huang[2], Donghua Shi[2], Jinmiao Lin[1], Jingyi Guo[1], Yiru Yang[3], Shilin Li[3*†] and Guorong Lyu[3*†]

Abstract

Background Fetal growth restriction (FGR) and late-onset preeclampsia (late-onset PE) reflect placental dysfunction but exhibit distinct maternal hemodynamics within the "maternal cardiovascular-placental-fetal unit".

Introduction Our objective was to investigate the correlation between fetal-placental Doppler indices and maternal cardiac function in pregnant women with late-onset PE or FGR.

Methods A total of 90 pregnant women at 35–39^{+6} weeks of gestation were enrolled and divided into three groups: Control ($n=30$), FGR ($n=30$), and late-onset PE ($n=30$). Doppler ultrasonography was used to measure uterine artery pulsatility indices(UtA-PI), umbilical artery pulsatility indices(UA-PI) Z-scores, and middle cerebral artery pulsatility indices(MCA-PI) Z-scores, alongside maternal hemodynamic parameters, including cardiac output (CO), peripheral vascular resistance (PVR), left ventricular mass (LVM), and left atrial anteroposterior diameter (LAAPD).The Kruskal-Wallis test was used to compare characteristics among the three groups. Spearman's rank correlation analysis was employed to assess relationships between maternal cardiac output/peripheral vascular resistance and fetal-placental Doppler indices in the three subgroups. Partial Spearman rank correlation analysis adjusting for maternal age and BMI was used to evaluate independent associations.

Results FGR neonates had the lowest birth weights ($p<0.05$). The FGR group showed reduced CO, LVM, LAAPD ($p<0.05$) but elevated PVR, UtA-PI, UA-PI Z-scores ($p<0.05$). Late-onset PE exhibited preserved cardiac function (CO, LVM, LAAPD comparable to controls, $p>0.05$) but significantly higher CO, LVM, LAAPD than FGR ($p<0.05$). No significant differences in MCA-PI Z-scores were observed across groups. UtA-PI negatively correlated with CO ($\rho=-0.396$, $p<0.001$) but positively with PVR ($\rho=0.371$, $p<0.001$). UA-PI Z-score negatively correlated with CO

†Shilin Li and Guorong Lyu contibuted equally to this work as corresponding authors.

*Correspondence:
Shilin Li
lslqz@fjmu.edu.cn
Guorong Lyu
lgr_fcus@sina.com

Full list of author information is available at the end of the article

(ρ=−0.257, $p=0.015$). However, MCA-PI Z-scores showed no correlation with CO and PVR.Notably, 90% of FGR cases clustered in the low-CO/high-UtA-PI quadrant.

Conclusions In direct response to our primary aim investigating maternal-fetal hemodynamic coupling, we conclude that: FGR manifests as maternal hemodynamic failure (low-CO/high-UtA-PI) causing placental hypoperfusion; Late-onset PE presents volume overload with preserved uteroplacental function; Dual UtA-PI and CO assessment provides phenotype-specific biomarkers to guide targeted therapy.

Keywords Cardiac output, Doppler ultrasonography, Fetal growth restriction, Late-onset preeclampsia

Introduction

Preeclampsia (PE), a multisystem disorder affecting 2–5% of pregnancies, remains a leading cause of maternal mortality, particularly in early-onset cases [1]. Clinically stratified into early-onset PE ($<34^{+0}$ weeks' gestation) and late-onset PE ($\geq 34^{+0}$ weeks' gestation), its pathogenesis remains debated between two main pathophysiological paradigms: placental origin and maternal cardiovascular etiology [1]. Kalafat et al. posit PE as a cardiovascular syndrome continuum, where early-onset PE primarily stems from structural/functional placental defects, while late-onset PE represents a "maternal-origin" phenotype. In this paradigm, preexisting maternal cardiovascular maladaptation– characterized by impaired cardiac load tolerance– precedes clinical manifestations, with placental dysfunction emerging as a secondary consequence of hemodynamic insufficiency [2]. Yagel et al. [3] further integrated this through a tripartite model of maternal-placental-fetal crosstalk, where disrupted vascular remodeling (maternal), perfusion anomalies (placental), or aberrant fetal signaling may collectively destabilize gestational homeostasis, culminating in PE syndrome.

We hypothesize that the core pathophysiological mechanism of FGR is placental hypoperfusion resulting from maternal hemodynamic failure (manifested as low CO and high PVR). In contrast, late-onset PE may primarily involve abnormal volume loading, with placental function remaining relatively functional.

Building upon these mechanistic insights, we recruited a prospective cohort of women at $35–39^{+6}$ weeks' gestation, stratified into three clinically defined groups: late-onset PE, FGR, and Controls. All participants underwent comprehensive cardiovascular profiling (including CO, PVR, and ventricular remodeling indices) coupled with fetal-placental Doppler ultrasonography (UA, UtA, and MCA pulsatility indices). This study aims to: (1) systematically compare maternal cardiovascular adaptations and fetal-placental hemodynamics across physiological and pathological pregnancies; (2) delineate late-onset PE-specific cardiac functional alterations (systolic/diastolic parameters); (3) establish clinically actionable correlations between maternal hemodynamics and placental perfusion indices. These objectives address critical knowledge gaps in tailoring management strategies for late-onset PE/FGR comorbidities.

Methods

A prospective cohort study was conducted from January 2023 to April 2024, enrolling 90 singleton pregnancies at 35^{+0} to 39^{+6} weeks of gestation who underwent antenatal care and delivery at our institution. Participants were categorized into three groups: Control ($n=30$), FGR ($n=30$), and late-onset PE ($n=30$). Inclusion criteria comprised non-smoking women aged 18 ~ 44 years without chronic hypertension, diabetes, renal diseases, or cardiac comorbidities. Exclusion criteria included multifetal gestations, fetal congenital anomalies, and maternal congenital heart disease or prior cardiac surgery.

PE was defined as new-onset hypertension (systolic blood pressure ≥ 140 mmHg and/or diastolic blood pressure ≥ 90 mmHg) after 20 weeks of gestation, combined with either proteinuria (≥ 0.3 g/24 h, protein/creatinine ratio ≥ 0.3, or dipstick ≥ 1+) or end-organ dysfunction (cardiopulmonary, hepatic, renal, hematologic, neurologic, or placental involvement) per ISSHP guidelines [4]. FGR was diagnosed per Delphi consensus criteria for late-onset fetal growth restriction (≥ 32 weeks), defined as meeting any of the following:

Abdominal circumference (AC) or estimated fetal weight (EFW) < 3rd percentile;

EFW or AC < 10th percentile;

Crossing > 2 quartiles in AC or EFW on growth trajectory charts;

Cerebroplacental ratio (CPR) < 5th percentile;

UA-PI > 95th percentile [5].

Gestational age was confirmed via first-trimester crown-rump length (11–13 weeks). All participants abstained from caffeine for ≥ 4 h and rested supine for 10 min prior to standardized cardiovascular assessments [6], including Doppler echocardiography-derived CO, PVR, LVM, and LAAPD. Fetal-placental Doppler pulsatility indices (UA-PI, UtA-PI, and MCA-PI) were concurrently measured. The study protocol was approved by the Ethics Committee of Jinjiang Hospital (No. jjsyyyxll-2022058), with written informed consent obtained from all participants.

Fetal-placental doppler ultrasonography

Ultrasound examinations were performed using two standardized systems: a Philips EPIQ Elite color Doppler ultrasonography system (S5-1 transducer, 3.0–5.0 MHz) and a GE Voluson E8 system (CL5-1 curvilinear transducer, 2.0–5.0 MHz). Fetal biometry included biparietal diameter, head circumference, abdominal circumference, and femur length measurements, with growth assessment standardized using the Hadlock reference charts.

UA evaluation

During fetal quiescence (absence of breathing movements), color Doppler was utilized to identify umbilical cord flow within amniotic fluid. Pulsed-wave Doppler sampling was performed on a free-floating umbilical arterial segment, maintaining an insonation angle < 20°. Spectral waveforms were acquired by automatic trace of ≥ 5 consecutive stable cardiac cycles, and the PI was calculated [7].

MCA protocol

The MCA was visualized in an axial transcerebral plane encompassing the thalamus and sphenoid wings. Color Doppler mapping identified the proximal MCA segment within the Circle of Willis. The sample gate was positioned at the proximal third of the MCA, near its origin from the internal carotid artery, with angle correction ≤ 10°. Three to ten consecutive waveforms were recorded under minimal transducer pressure to avoid hemodynamic artifact, and MCA-PI was derived [7].

UtA assessment

Bilateral uterine arteries were localized at their crossover points with the external iliac vessels. Spectral Doppler traces were acquired 1 cm distal to the crossover point, with PI values averaged between left and right arteries. Angle of insonation was maintained < 30° throughout measurements [7].

Maternal cardiovascular assessment

Maternal cardiovascular evaluations were systematically performed with participants in the left lateral decubitus position to minimize aortocaval compression. Transthoracic echocardiography (TTE) was utilized to derive CO through pulsed-wave Doppler measurements of the left ventricular outflow tract (LVOT) velocity-time integral (VTI). Stroke volume (SV) was calculated as the product of LVOT cross-sectional area and VTI, with CO subsequently determined by multiplying SV by heart rate (HR). LVM was quantified using the Devereux formula:

$$\mathrm{LVM\,(g)} = 0.8 \times \left\{1.04 \times \left[(\mathrm{IVSd} + \mathrm{LVIDd} + \mathrm{PWd})^3 - \mathrm{LVIDd}^3\right]\right\} + 0.6$$

where IVSd, LVIDd, and PWd represent interventricular septal thickness, left ventricular internal diameter in diastole, and posterior wall thickness at end-diastole, respectively [8]. LAAPD was measured in the parasternal long-axis view during end-systole. Blood pressure measurements were obtained using an automated oscillometric device (Omron HBP-9020) on the right arm after 5 min of standing rest [9], with mean arterial pressure (MAP) calculated as:

$$\mathrm{MAP\,(mmHg)} = \mathrm{Diastolic\ BP} + (\mathrm{Systolic\ SBP} - \mathrm{Diastolic\ BP})/3$$

Peripheral vascular resistance (PVR, dynes·s/cm^5) was derived from the relationship:

$$\mathrm{PVR} = \mathrm{MAP} \times 80/\mathrm{CO}$$

where CO is expressed in L/min [10].

Given that all enrolled participants were at 35^{+0} to 39^{+6} weeks' gestation, the following parameters were not adjusted for gestational age: CO, PVR, LAAPD, LVM, and UtA-PI [10, 11]. In contrast, gestational age-specific Z-scores were utilized for both UA-PI and MCA-PI.Z-scores for UA-PI and MCA-PI were calculated based on gestational age-specific reference ranges [12].

Statistical analysis

Data were analyzed using SPSS 29.0 (IBM Corp.) Continuous variables are presented as median and interquartile range (IQR). Intergroup differences among the three cohorts were assessed by the Kruskal-Wallis test. Spearman's rank correlation analysis was employed to assess relationships between maternal cardiac output/peripheral vascular resistance and fetal-placental Doppler indices in the three subgroups. Partial Spearman rank correlation analysis adjusting for maternal age and BMI was used to evaluate independent associations. Statistical significance was defined as a two-tailed $p < 0.05$.

Results

Comparative analysis of clinical characteristics, fetal-placental doppler indices, and maternal cardiac parameters

No significant differences were observed in maternal age or gestational age across the three groups. However, women with late-onset PE exhibited significantly higher BMI compared to both the controls and FGR groups ($p < 0.05$) (Table 1). Hemodynamically, the FGR group exhibited distinct alterations compared to both controls and the late-onset PE group: Cardiac parameters(LAAPD, LVM, CO) were significantly reduced in FGR vs. controls and late-onset PE ($p < 0.05$); Placental resistance markers

Table 1 Comparative analysis of clinical characteristics, Fetal-Placental doppler indices, and maternal cardiac function parameters across study groups

characteristic	Control ($n=30$)	Late-Onset PE ($n=30$)	FGR ($n=30$)	*p*-Value
Maternal Age (years)	28.50(25.75–32.25)	29.00(26.75–30.5)	27.00(24.75–29.00)	0.075
BMI (kg/m^2)	26.55(23.88–28.13)	30.50(28.03–32.53)[ab]	24.85(23.10–27.53)	<0.001
Gestational Age at Delivery (weeks)	36.60(36.20–37.50)	37.15(36.90–38.10)	37.55(36.25–38.60)	0.056
UA-PI Z-scores	0.17(−0.29-0.67)	0.66(0.19–1.22)[b]	1.20(0.69–1.79) [a]	<0.001
MCA-PI Z-scores	−0.18(−0.59-0.49)	−0.23(−0.73-0.32)	−0.08(−0.61-1.05)	0.523
UtA-PI	0.80(0.64–0.88)	0.88(0.79–0.98)[b]	1.12(1.06–1.22)[a]	<0.001
Neonatal Birth Weight (grams)	3255.00(3082.50–3562.50)	3067.50(2768.75–3277.50)[b]	2445.00(2332.50–2672.50)[a]	<0.001
CO (L/min)	4.79(4.07–5.73)	5.70(4.78–6.33)[b]	3.85(3.50–4.10)[a]	<0.001
PVR (dyn·s/cm^5)	1402.15(1036.48–1682.05)	1595.40(1430.41–1906.00)[b]	1859.67(1687.59–2020.54)[a]	<0.001
LVM (g)	126.00(105.25–131.75)	130.00(119.75–135.25)[b]	109.00(104.00–118.00)[a]	<0.001
LAAPD (mm)	34.00(32.00–35.00)	34.50(33.00–35.08)[b]	30.00(29.00–31.25)[a]	<0.001

Notes: Data are presented as median (interquartile range); Superscript letters indicate statistically significant differences ($p<0.05$)

[a]Significantly different from Normal Pregnancy Group ($p<0.05$)

[b]Significantly different from FGR Group ($p<0.05$)

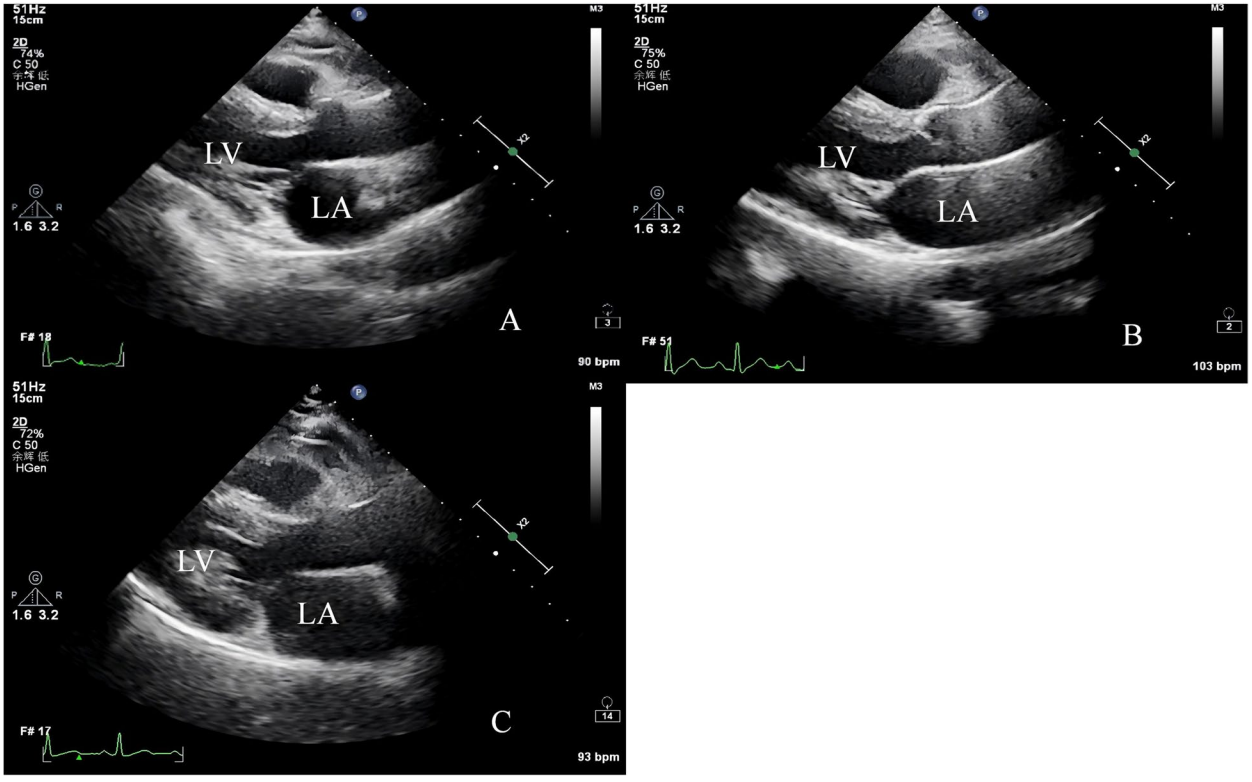

Fig. 1 Echocardiographic Characterization of LAAPD Across Study Groups A Normal Pregnancy Group, Gestational age: 38 weeks, Maternal age: 24 years, LAAPD: 32 mm.B FGR Group, Gestational age: 36 weeks, Maternal age: 31 years, LAAPD: 31 mm.C Late-Onset PE Group, Gestational age: 36^{+1} weeks, Maternal age: 30 years, LAAPD: 39 mm

(PVR, UtA-PI, UA-PI Z-scores) were significantly elevated in FGR vs. both groups ($p<0.05$).

Conversely, late-onset PE demonstrated: Cardiac dimensions/hemodynamics comparable to controls; Placental resistance markers (PVR, UtA-PI, UA-PI Z-scores) similar to controls but significantly lower than FGR ($p<0.05$). No significant differences in MCA-PI Z-scores were observed across groups (Table 1). Figure 1 illustrates representative echocardiographic measurements of LAAPD.

Correlations between UtA-PI/UA-PI zscore/MCA-PI zscore and maternal CO/PVR

In the total cohort, UtA-PI demonstrated a significant negative correlation with CO(ρ = −0.396, $p<0.001$, 95% CI −0.550 to −0.209), UtA-PI showed a significant

Table 2 Partial spearman's correlation adjusted for age and BMI

Variable pair	Unadjusted ρ (*p*-value)	Unadjusted 95% CI	Adjusted ρ (*p*-value)	Adjusted 95% CI
UtA-PI vs. CO	−0.396(<0.001)*	[−0.550, −0.209]	−0.354(<0.001)*	[−0.507, −0.165]
UtA-PI vs. PVR	0.371(<0.001)*	[0.183, 0.517]	0.327(0.002)*	[0.127, 0.502]
UA-PI Zscore vs. CO	−0.257(0.015)*	[−0.452, −0.045]	−0.252(0.018)*	[−0.435, −0.039]
UA-PI Zscore vs. PVR	0.158(0.136)	[−0.056, 0.351]	0.128(0.234)	[−0.095, 0.329]
MCA-PI Zscore vs. CO	−0.046(0.667)	[−0.251, 0.164]	−0.151(0.160)	[−0.359, 0.063]
MCA-PI Zscore vs. PVR	0.075(0.485)	[−0.129, 0.287]	0.124(0.250)	[−0.082, 0.314]

Notes:ρ: Spearman's correlation coefficient; Unadjusted: crude correlation without covariate adjustment; Adjusted: adjusted for maternal age and BMI

CI Confidence interval, *BCa* Bootstrap with 1,000 resamples

*Statistical significance was defined as a two-tailed $p < 0.05$

positive correlation with PVR (ρ = 0.371, $p < 0.001$, 95% CI 0.183 to 0.517), UA-PI Zscore showed a significant negative correlation with CO (ρ = −0.257, $p = 0.015$, 95% CI −0.452 to −0.045).However, MCA-PI Z-scores showed no correlation with CO and PVR (Table 2).

Subgroup-specific correlations

Partial Spearman analysis across the three subgroups revealed a significant positive correlation between UtA-PI and CO in the FGR group (ρ = 0.463, $p = 0.010$; 95% CI: 0.112 to 0.711). This association persisted after adjustment for maternal age and BMI (Table 3). Conversely, UA-PI Z-score showed a negative correlation with PVR in the FGR group (ρ=−0.381, $p = 0.038$; 95% CI: −0.658 to −0.013). However, no significant correlation remained after adjusting for age and BMI (Table 3). Neither the control nor late-onset PE groups demonstrated significant associations between UtA-PI/UA-PI Z-scores and maternal hemodynamic parameters. Scatter plots of UtA-PI versus CO (Fig. 2) revealed clustering of 27/30 (90%) FGR cases in the low-CO/high-UtA-PI quadrant, compared to only 1/30 (3.3%) controls and 1/30 (3.3%) late-onset PE cases (Fig. 2).

Discussion

Focusing on our core objective to correlate fetal-placental Doppler indices with maternal cardiac function, we observed that during normal pregnancy, maternal cardiovascular adaptation involves increased blood volume and CO to compensate for physiological reductions in PVR, accompanied by adaptive LVM augmentation [13, 14], thereby ensuring adequate fetoplacental perfusion [15]. Our findings reveal distinct maternal hemodynamic-placental coupling patterns across pathological pregnancy states: The FGR cohort demonstrated reduced CO, elevated PVR, and diminished LVM, suggesting inadequate cardiovascular compensation leading to placental hypoperfusion. In contrast, the late-onset PE group exhibited hemodynamic profiles (CO, PVR) comparable to normal pregnancies but displayed significantly greater LAAPD and LVM than the FGR group, indicative of divergent cardiac remodeling trajectories, suggesting their cardiovascular compensatory capacity remains intact [16]. Placental circulatory analysis showed that in the FGR group, both UtA-PI and UA-PI Z-scores were significantly elevated compared to the control and late-onset PE groups, suggesting that placental hypoperfusion may directly impair fetal development. These collective findings indicate a potential pathological coupling mechanism between maternal hemodynamic dysfunction and placental insufficiency [16, 17].

The placenta, as the central interface for maternal-fetal exchange, plays a pivotal role in pregnancy homeostasis, with its dysfunction directly implicated in pathological outcomes such as FGR and PE [18]. It was observed that UtA-PI inversely correlated with maternal CO, but positively with PVR. Furthermore, most cases in the FGR group clustered within the region characterized by high UtA-PI and low CO. UtA-PI inversely correlated with maternal CO but positively with PVR. Crucially,

Table 3 Unadjusted and adjusted spearman correlations (ρ) for maternal age and BMI across study groups

Variable pair	Group	Unadjusted ρ (*p*-value)	Unadjusted 95% CI	Adjusted ρ (*p*-value)	Adjusted 95% CI
UtA-PI vs. CO	Control Group	0.105(0.581)	[−0.244, 0.438]	−0.026(0.895)	[−0.410, 0.340]
	Late-Onset PE Group	0.038(0.840)	[−0.337, 0.400]	0.143(0.469)	[−0.242, 0.472]
	FGR Group	0.463(0.010)*	[0.112, 0.743]	0.428(0.023)*	[0.142, 0.699]
UA-PI Zscore vs. PVR	Control Group	0.016(0.932)	[−0.381, 0.425]	0.030(0.879)	[−0.321, 0.405]
	Late-Onset PE Group	−0.193(0.307)	[−0.519, 0.169]	−0.214(0.274)	[−0.549, 0.133]
	FGR Group	−0.381(0.038)*	[−0.606, −0.076]	−0.334(0.082)	[−0.619,−0.027]

Notes: *PE* Preeclampsia, *FGR* Fetal Growth Restriction ρ Spearman's correlation coefficient, Unadjusted: crude correlation without covariate adjustment; Adjusted: adjusted for maternal age and BMI, *CI* Confidence interval, *BCa* bootstrap with 1,000 resamples

*Statistical significance was defined as a two-tailed $p < 0.05$

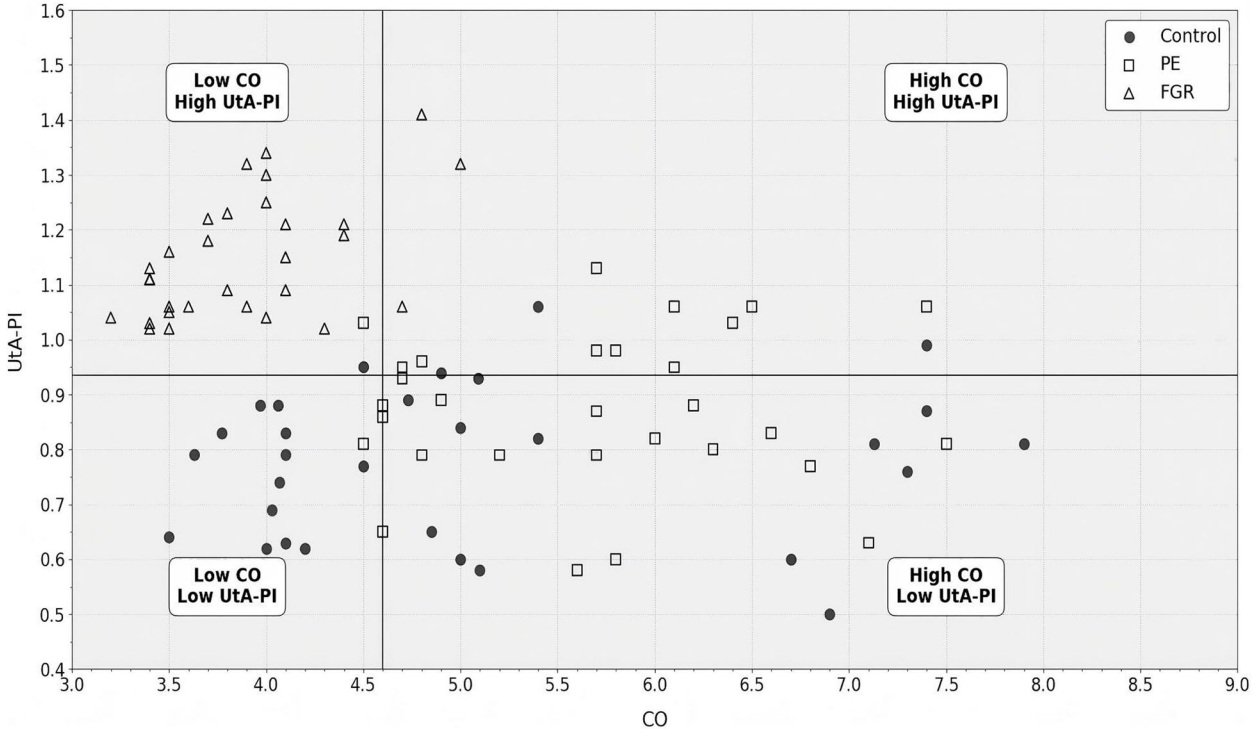

Fig. 2 Scatter plot depicting the distribution of UtA-PI versus CO in 90 cases (30 FGR, 30 Control, and 30 late-onset PE). FGR cases predominantly clustered in the high-UtA-PI/low-CO quadrant. Additionally, 90% of FGR cases fall within high-UtA-PI/low-CO quadrant. Notes: High UtA-PI/Low CO quadrant (UtA-PI > 1.0, CO < 4.0 L/min)

90% of FGR cases clustered in the high-UtA-PI/low-CO quadrant, indicating a vicious cycle: diminished cardiac output elevates placental resistance, exacerbating fetal hypoxia and endothelial dysfunction which further reduces CO [19–23].

Notably, this study identified 6 FGR cases complicated by early-onset PE, with the onset of PE consistently preceding the development of FGR. This temporal sequence suggests that early-onset PE and FGR may share a common early pathological basis of impaired spiral artery remodeling in the placenta. In contrast, placental injury in late-onset PE likely stems from dysregulated villous perfusion secondary to uterine volume overload, primarily manifesting as placental focal ischemia, while the maternal cardiovascular system remains compensatory. This points to the potential existence of phenotype-specific pathological mechanisms in PE [24–26]. Therefore, the interaction between maternal hemodynamic abnormalities and placental dysfunction may offer novel avenues for early warning and intervention in pathological pregnancies. Farsetti et al. [27] found that in cases of early-onset FGR with maternal hemodynamic abnormalities, the use of a nitric oxide donor (glyceryl trinitrate transdermal patch) combined with oral rehydration reduced systemic vascular resistance, increased cardiac output, significantly enhanced umbilical venous blood flow, improved fetal oxygenation and provided neuroprotective effects, leading to a lower incidence of PE. Conversely, Yagel et al. [28] proposed that PE treatment strategies should focus on maternal hemodynamic profiles. For late-onset PE, they recommend using α/β-adrenergic blockers (e.g., labetalol) to reduce cardiac output, control blood pressure, and alleviate cardiac load– a treatment approach distinct from the use of NO donors to improve low cardiac output in early-onset PE.So for FGR cases with low CO/high UtA-PI, nitric oxide donors may improve placental perfusion by reducing vascular resistance. Conversely, in late-onset PE with preserved CO, β-blockers (e.g., labetalol) could optimize cardiac load without compromising fetal supply.

Interestingly, we found that the maternal hemodynamic characteristics across the three groups showed no significant correlation with the fetal MCA-PI Z-scores. This suggests that the hypoxic pathway may not serve as the primary mediator of these interactions. Our null findings regarding MCA-PI and maternal hemodynamics align with Valensise et al. [29], suggesting that chronic placental insufficiency may decouple fetal cerebral Doppler regulation from maternal cardiovascular adaptations. While Masini et al. [30] reported MCA-PI associations with maternal hemodynamics, our data align with Valensise et al. in showing no correlation. This may reflect differences in placental insufficiency timing (acute vs. chronic). Further studies are warranted. Within the FGR

group, our univariate analysis revealed a significant association between maternal PVR and the UA-PI. However, after controlling for maternal age and BMI, this association lost significance. This may partially reflect the broad influence of maternal metabolic factors on the vascular system. This finding underscores the necessity for future research on utero-peripheral vascular coupling mechanisms to fully account for the regulatory role of maternal metabolic status [31, 32].

This study has several limitations: First, the exclusion of early-onset PE cohorts precludes direct hemodynamic comparisons across PE subtypes. Second, potential birth weight bias in the FGR group due to clinical interventions necessitates validation through prospective controlled studies. Third, the lack of dynamic cardiac functional assessments (e.g., diastolic functional indices) may underestimate the impact of subclinical myocardial dysfunction.Future large-scale longitudinal cohorts are needed to both establish high-risk hemodynamic thresholds for FGR and validate early-pregnancy predictors.

In conclusion, our study confirms a pathophysiological dichotomy: Fetal growth restriction (FGR) is driven by maternal hemodynamic failure (low cardiac output and high uterine artery resistance), directly causing placental hypoperfusion and fetal nutrient restriction. In contrast, late-onset preeclampsia involves volume overload with preserved placental function. This distinction supports dual UtA-PI and CO assessment as a phenotype-specific biomarker profile to guide targeted therapy: Nitric oxide donors for FGR to augment placental perfusion, and β-blockers for late-onset PE to optimize cardiac load.

Declaration of generative AI and AI-assisted technologies in the writing process

During the preparation of this work the authors used DeepSeek's AI tools in order to assist in English translation of manuscripts. After using this tool, the authors reviewed and edited the content as needed and take full responsibility for the content of the publication.

Supplementary Information

The online version contains supplementary material available at https://doi.org/10.1186/s12884-025-07848-x.

Supplementary Material 1.

Supplementary Material 2.

Supplementary Material 3.

Supplementary Material 4.

Supplementary Material 5.

Acknowledgements

Acknowledgements We sincerely thank the obstetric and ultrasound medicine staff at Jinjiang Municipal Hospital(Shanghai Sixth People 's Hospital Fujian) for their assistance in patient recruitment and data collection. We are grateful to Professor Guorong Lyu (The Second Affiliated Hospital of Fujian Medical University) for her expert advice on experimental design. We also acknowledge the DeepSeek's AI tools for English translation and language polishing of this manuscript.Finally, we extend our heartfelt gratitude to all the pregnant women who participated in this study, as well as their families, for their cooperation and trust.

Authors' contributions

Author Contributions: Y.L.,G.R.: Conceptualization, Methodology, Writing– Original Draft Y.R.,Y.L.: Formal Analysis, Data Curation. G.R.,S.L.: Writing– Review & EditingY.L.,M.H.: Funding Acquisition. J.M.,J.Y.,D.H.,M.H.:Data collection, Investigation, Data Curation.All authors read and approved the final manuscript.

Funding

This work was supported by the Joint funds for the innovation of science and technology, Fujian Province (Grant No. 2024Y9473 and 2023Y9231), Quanzhou CityScience & Technology Program of China (Grant No. 2023N021S), and JinJiang Municipal Hospital (Shanghai sixth People's Hospital Fujian) technology project (Grant No. 2022LC01).

Data availability

The datasets generated and analyzed during this study are not publicly available due to patient confidentiality and institutional data protection policies. However, anonymized data supporting the findings are available from the corresponding author (Dr. Guorong Lyu, email-lgr_feus@sina.com) upon reasonable request. Requests will be reviewed by the ethics committee to ensure compliance with privacy regulations.

Declarations

Ethics approval and consent to participate

This study was approved by the Ethics Committee of Jinjiang Municipal Hospital (Approval No. jjsyyyxll-2022058). Written informed consent was obtained from all participants prior to their inclusion in the study. All procedures followed the ethical standards of the 1964 Helsinki Declaration and its later amendments.

Consent for publication

All participants provided written consent for the publication of anonymized data. Identifiable information (e.g., images, names) has been removed to protect participant privacy.

Competing interests

The authors declare no competing interests.

Author details

[1]Department of Ultrasound Medicine, Jinjiang Municipal Hospital (Shanghai Sixth People's Hospital Fujian), Quanzhou 362000, Fujian, China
[2]Department of Obstetrics, Jinjiang Municipal Hospital (Shanghai Sixth People's Hospital Fujian), Quanzhou 362000, Fujian, China
[3]Department of Ultrasound Medicine, The Second Affiliated Hospital of Fujian Medical University, Quanzhou 362000, Fujian, China

Received: 26 March 2025 / Accepted: 17 June 2025
Published online: 10 July 2025

References

1. Poon LC, Shennan A, Hyett JA, Kapur A, Hod M, McIntyre HD, et al. The international federation of gynecology and obstetrics (FIGO) initiative on pre-eclampsia: a pragmatic guide for first-trimester screening and prevention. Int J Gynaecol Obstet. 2019;145(Suppl 1):1–33. https://doi.org/10.1002/ijgo.12802.
2. Kalafat E, Thilaganathan B. Cardiovascular origins of preeclampsia. Curr Opin Obstet Gynecol. 2017;29(6):383–9. https://doi.org/10.1097/GCO.0000000000000412.
3. Yagel S, Cohen SM, Goldman-Wohl D. An integrated model of preeclampsia: a syndrome of the maternal-placental-fetal array. Am J Obstet Gynecol. 2022;226(2S):S963–72. https://doi.org/10.1016/j.ajog.2021.12.003.

4. Hypertensive Disorders in Pregnancy Group, Chinese Society of Obstetrics and Gynecology. Guidelines for diagnosis and management of hypertensive disorders in pregnancy (2020). Chin J Obstet Gynecol. 2020;55(4):227–37. [In Chinese].
5. Gordijn SJ, Beune IM, Thilaganathan B, et al. Consensus definition of fetal growth restriction: a Delphi procedure. Ultrasound Obstet Gynecol. 2016;48(3):333–9. https://doi.org/10.1002/uog.15884.
6. Ultrasound Society of Chinese Medical Association. Guidelines for echocardiographic measurements in Chinese adults. Chin J Ultrasonogr. 2016;25(8):645–66. [In Chinese].
7. Bhide A, Acharya G, Baschat A, Bilardo CM, Brezinka C, Cafici D, et al. ISUOG practice guidelines (updated): use of doppler velocimetry in obstetrics. Ultrasound Obstet Gynecol. 2021;58(2):331–9. https://doi.org/10.1002/uog.23698.
8. Devereux RB, Casale PN, Kligfield P, Eisenberg RR, Miller D, Campo E, et al. Performance of primary and derived M-mode echocardiographic measurements for detection of left ventricular hypertrophy. Am J Cardiol. 1986;57(15):1388–93. https://doi.org/10.1016/0002-9149(86)90215-4.
9. de Greeff A, Beg Z, Gangji Z, Dorney E, Shennan AH. Accuracy of oscillometry in pregnancy and preeclampsia: OMRON-MIT versus OMRON-M7. Blood Press Monit. 2009;14(1):37–40. https://doi.org/10.1097/MBP.0b013e3283262f31.
10. Valensise H, Novelli GP, Vasapollo B, Di Ruzza L, Giorgi G, Galante A, et al. Maternal cardiac function and uteroplacental resistances: a Doppler-echocardiographic study. Ultrasound Obstet Gynecol. 2000;15(6):487–97. https://doi.org/10.1046/j.1469-0705.2000.00134.x.
11. Tay J, Foo L, Masini G, et al. Early and late preeclampsia are characterized by high cardiac output, but in the presence of fetal growth restriction, cardiac output is low: insights from a prospective study. Am J Obstet Gynecol. 2018;218(5):517. https://doi.org/10.1016/j.ajog.2018.02.007.
12. Parra-Cordero M, Lees C, Missfelder-Lobos H, et al. Fetal arterial and venous doppler pulsatility index and time averaged velocity ranges. Prenat Diagn. 2007;27(13):1251–7. https://doi.org/10.1002/pd.1868.
13. Fok WY, Chan LY, Wong JT, Yu CM, Lau TK. Left ventricular diastolic function during normal pregnancy. Ultrasound Obstet Gynecol. 2006;28(6):789–93. https://doi.org/10.1002/uog.3813.
14. van Zijl MD, Koullali B, Mol BWJ, Oudijk MA, van der Post JAM, Groen H, et al. Uterine artery doppler for preterm birth prediction. Acta Obstet Gynecol Scand. 2020;99(4):494–502. https://doi.org/10.1111/aogs.13772.
15. Small HY, Morgan H, Beattie E, Griffin S, Indahl M, Delles C, et al. Uterine artery remodeling in hypertensive rats. Placenta. 2016;37:34–44. https://doi.org/10.1016/j.placenta.2015.12.002.
16. Masini G, Foo LF, Tay J, Wilkinson IB, McEniery CM, Bennett PR, et al. Preeclampsia phenotypes and treatment strategies. Am J Obstet Gynecol. 2022;226(2S):S1006–18. https://doi.org/10.1016/j.ajog.2021.11.1350.
17. Maseliene T, Zukiene G, Laurinaviciene A, Breskuviene D, Ramasauskaite D, Dzenkeviciute V. Alterations in maternal cardiovascular parameters and their impact on uterine and fetal circulation in hypertensive pregnancies and fetal growth restriction. Int J Cardiol Cardiovasc Risk Prev. 2024;22:200316. https://doi.org/10.1016/j.ijcrp.2024.200316.
18. Baschat AA. Fetal responses to placental insufficiency. BJOG. 2004;111(10):1031–41. https://doi.org/10.1111/j.1471-0528.2004.00264.x.
19. Magee LA, Nicolaides KH, von Dadelszen P, Preeclampsia. N Engl J Med. 2022;386(19):1817–32. https://doi.org/10.1056/NEJMra2109523.
20. Shah DA, Khalil RA. Placental ischemia and vascular dysfunction. Biochem Pharmacol. 2015;95(4):211–26. https://doi.org/10.1016/j.bcp.2015.04.012.
21. Tay J, Masini G, McEniery CM, Bennett PR, Wilkinson IB, Lees CC. Placental doppler and maternal cardiovascular function. Am J Obstet Gynecol. 2019;220(1):e961–8. https://doi.org/10.1016/j.ajog.2018.10.086.
22. Stampalija T, Monasta L, Di Martino DD, Casati D, Sassi F, Parazzini F, et al. Uterine artery doppler in hypertensive pregnancy. J Matern Fetal Neonatal Med. 2019;32(7):1191–9. https://doi.org/10.1080/14767058.2017.1402878.
23. Lees CC, Stampalija T, Baschat A, da Silva Costa F, Ferrazzi E, Figueras F, et al. ISUOG guidelines: fetal growth restriction. Ultrasound Obstet Gynecol. 2020;56(2):298–312. https://doi.org/10.1002/uog.22134.
24. Redman CWG, Staff AC, Roberts JM. Syncytiotrophoblast stress in preeclampsia. Am J Obstet Gynecol. 2022;226(2S):S907–27. https://doi.org/10.1016/j.ajog.2021.11.1355.
25. Staff AC. The two-stage model of preeclampsia. J Reprod Immunol. 2019;134–135:1–10. https://doi.org/10.1016/j.jri.2019.07.004.
26. Valensise H, Vasapollo B, Gagliardi G, et al. Hemodynamic States in early and late preeclampsia. Hypertension. 2008;52(5):873–80. https://doi.org/10.1161/HYPERTENSIONAHA.108.112516.
27. Farsetti D, Pometti F, Vasapollo B, et al. Nitric oxide donor increases umbilical vein blood flow and fetal oxygenation in fetal growth restriction. A pilot study. Placenta. 2024;151:59–66. https://doi.org/10.1016/j.placenta.2024.04.014.
28. Yagel S, Cohen SM, Admati I, Cuckle H, Meiri H. Preeclampsia type I and type II. Am J Obstet Gynecol MFM. 2023;5(12):101203. https://doi.org/10.1016/j.ajogmf.2023.101203.
29. Valensise H, Farsetti D, Pometti F, et al. The cardiac-fetal-placental unit: fetal umbilical vein flow rate is linked to the maternal cardiac profile in fetal growth restriction. Am J Obstet Gynecol. 2023;228(2):222..e1-222.e12.
30. Masini G, Tay J, McEniery CM, et al. Maternal cardiovascular dysfunction is associated with hypoxic cerebral and umbilical Doppler changes. J Clin Med. 2020;9(9): 2891. https://doi.org/10.3390/jcm9092891.
31. Wiertsema CJ, Mensink-Bout SM, Duijts L, Mulders AGMGJ, et al. Associations of DASH diet in pregnancy with blood pressure patterns, placental hemodynamics, and gestational hypertensive disorders. J Am Heart Assoc. 2021;10(1):e017503. https://doi.org/10.1161/JAHA.120.017503.
32. Li Y, Han B, Salmeron AG, Bai J, et al. Estrogen-induced uterine vasodilation in pregnancy and preeclampsia. Maternal-Fetal Medicine. 2021;4(1):52–60. https://doi.org/10.1097/FM9.0000000000000132.

Publisher's Note